ELSEVIER

Biochimica et Biophysica Acta 1297 (1996) 17–27

BBA Biochimica et Biophysica Acta

Analysis of wild-type and mutant aspartate aminotransferases using integrated rate equations

Martin R. Schiller *, Leonard D. Holmes [1], Elizabeth A. Boeker

Department of Chemistry and Biochemistry, Utah State University, Logan, UT 84322, USA

Received 23 October 1995; revised 16 January 1996; accepted 9 May 1996

Abstract

A general integrated rate equation was fit to reaction progress curves catalyzed by wild-type *E. coli* aspartate aminotransferase and the site-specific mutant enzymes, H193Q and Y70F. A nonlinear step-regression code, revised for this study selected from all kinetic constants in a general integrated rate equation for all unbranched enzyme mechanisms with stoichiometries upto two substrates and two products including terms for substrate inhibitions and that of an exogenous inhibitor. For each aspartate aminotransferase enzyme studied only kinetic constants consistent with a substituted enzyme mechanism were found statistically significant, thus the enzyme mechanism and sources of inhibition were determined objectively by statistics. The kinetic constants for wild-type and Y70F aspartate aminotransferase were similar to those previously reported indicating the validity of the integrated rate equation analysis. Minor changes in kinetic constants were observed for the H193Q mutant enzyme suggesting that the catalytic effects of the electrostatic hydrogen bonding network extending from the pyridine nitrogen of the cofactor through Asp-222, His-143, and His-189 ends prior to His-193.

Keywords: Nonlinear regression; Progress curve; Substrate inhibition; Correlation; Integrated rate equation

1. Introduction

An integrated rate equation modeling an enzymatic reaction was first presented by Henri [1]. This equation, more familiarly known in the derivative form as the Michaelis–Menten equation [2], predicts the substrate conversion rate of the simplest enzyme catalyzed reaction. Integrated rate equations found limited application in the decades succeeding Henri's initial kinetic characterization of an enzyme catalyzed reaction [3–5]. While kinetic study of noncatalyzed chemical reactions commonly utilizes integrated rate equations, enzyme-catalyzed reactions have been approached largely by fitting transformations of derivative rate equations to initial rate data as set forth by Alberty [6,7] and Cleland [8–10]. More recently, several enzymatic systems have been analyzed with mechanism-specific integrated rate equations [12–20], and progress curves catalyzed by glutamate dehydrogenase have been analyzed by numerical integration [11]. Derivative rate equations for all unbranched enzyme mechanism with stoichiometries of upto two substrates and two products were combined and integrated creating a *general* integrated rate equation [21–23]. The significance of kinetic constants in this general equation determines the enzymatic mechanism. This rate equation or shorter versions were used to analyze reactions catalyzed by arginine decarboxylase (ADC; [24,25]) and lactate dehydrogenase (LDH; [26]).

The statistical procedures used in the integrated rate equation analysis of ADC resulted in multiple prediction of some kinetic constants which varied by more than their standard deviations. In the integrated rate equation analysis of LDH, the Theorell–Chance and ordered ternary-complex mechanisms could not be distinguished because the significance of some constants was dependent on the weighting scheme used.

Abbreviations: LDH, lactate dehydrogenase; AAT, aspartate aminotransferase; MDH, malate dehydrogenase; PLP, pyridoxal phosphate; PMP, pyridoxamine phosphate; NADH, reduced nicotine adenine dinucleotide.

* Corresponding author. Present address: Departments of Neuroscience and Physiology, Johns Hopkins University School of Medicine, Baltimore, MD 21205, USA. Fax: +1 (410) 9550681; e-mail: schiller@welchlink.welch.jhu.edu.

[1] Present address: Department of Physical Science, Pembroke State University, Pembroke, NC 28372, USA.

PII S0167-4838(96)00083-0

We report the analysis of progress curves catalyzed by aspartate aminotransferase (AAT) with a revised regression analysis which resolved problems encountered in the study of ADC and LDH. The integrated rate equation was factored for 'J' constants as suggested by Duggleby and Wood [18] and all progress curve data were simultaneously fit in one regression. We have also expanded the general integrated rate equation to account for substrate inhibition which reduced the fitting error for progress curves catalyzed by AAT.

Analysis of the well studied wild-type, and Y70F site-specific mutant AATs provided a control for the revised regression method. Kinetic constants determined from reactions catalyzed by the H193Q site-specific mutant revealed little change when compared to wild-type AAT suggesting that residue His-193 of the hydrogen bonding network extending from the pyridine nitrogen of the cofactor has no significant role in catalysis.

2. Materials and methods

2.1. Notation

Concentrations of substrate and product are A, B, P, and Q (instantaneous) and A_0, B_0, P_0, and Q_0 (initial); chemical abbreviations are: aspartate, A; α-ketoglutarate, B; oxaloacetate, P; glutamate, Q; AAT inhibitor malate, M; pyridoxal-phosphate, PLP; pyridoxamine-phosphate, PMP; AAT-PLP complex, E; AAT-PMP complex, F. A 'data set' is a group of progress curves having different enzyme, initial substrate, and product concentrations. Equation abbreviations are; net change in product concentration ($P - P_0$) at time t; ΔP, an individual measurement, $_i$; a best fit value, $\hat{}$. The constants 'J' and 'C' were as previously defined [21–23,26]. The enzyme concentration (e_0) and turnover number k_{cat} were as defined by the Nomenclature Committee of the International Union of Biochemistry [27].

2.2. Materials

L-Aspartic acid, L-glutamic acid, oxaloacetic acid, α-ketoglutarate, NADH (reduced nicotine adenine dinucleotide), PLP, PMP, L-cysteine sulfinic acid, β-bromopyruvic acid, Hepes free acid (*N*-2-hydroxyethylpiperizine-*N'*-2-ethanesulfonic acid), crystalline bovine serum albumin, and bovine heart malate dehydrogenase (MDH; EC 1.1.1.37) were from Sigma (St. Louis, MO). All other chemicals were reagent grade. Recombinant *E. coli* strains expressing wild-type, and site-specific mutants, Y70F and H193Q, *E. coli* AAT proteins were gifts from the laboratory of Dr. Jack F. Kirsch (University of California, Berkeley).

2.3. Enzyme assays, enzyme preparation, and progress curves

All assays and progress curves were executed in a thermostated, water-jacketed cell holder of a Cary 219 spectrophotometer at 25°C. Analog data were collected with an Apple 2e computer and converted to IBM format using the software package UNIFORM 2.14 (Microsolutions, IL, USA). AAT catalyzed reaction progress curves and activity assays were monitored using a coupled assay; the AAT reaction product, oxaloacetate was reduced to malate by NADH, catalyzed by malate dehydrogenase (MDH; [28]). The coupled assay provided continuous spectrophotometric measurement and pushed the AAT reaction to completion.

Wild-type and mutant AATs were purified as described by Cronin and Kirsch [29]. Protein concentrations were measured spectrophotometrically at 205 nm [30]. The coupling enzyme, MDH, contained residual AAT activity which was inactivated using β-bromopyruvate and cysteine sulfinate as previously described [31]. MDH activity was measured by following the decrease in NADH absorbance at 340 nm as described in the Worthington Enzymes Manual [32]; the MDH was concentrated by dehydration in dialysis bags at 4°C using Sephadex G-100 as a hydroscopic agent.

AAT progress curve reactions contained 0.1 mg/ml bovine serum albumin, 0.2 or 7.0 mM NADH, 10 μM PLP (1.0 mM PMP for Y70F catalyzed reactions), 20 μmol/min/ml MDH, 0.01–60 μmol/min/ml AAT, and 0.1 M Hepes-KOH (pH 7.4). Aspartate, α-ketoglutarate, and glutamate concentrations are defined in Table 1. All progress curves reached equilibrium in 2 to 45 min and points were collected every 2 s. Controls for the MDH coupled AAT assay showed coupling enzyme saturation, no NAD^+ and NADH inhibition of AAT, no change in pH, and exhaustion of the limiting substrate. For wild-type and mutant AATs, these controls were further tested for several representative progress curves using Selwyn's test of enzyme inactivation [33] which revealed no inactivation for any progress curve. For each progress curve, the limiting and nonlimiting substrate concentrations were determined spectrophotometrically using the MDH coupled assay. The concentration of the reaction product, glutamate, at time 0 was calculated based on dilution of a stock solution measured using a Beckman System 6300 high-pressure chromatography amino-acid analyzer.

For progress curves where the limiting substrate concentration was less than 0.15 mM, oxidation of NADH was

Table 1
Data set substrate and product concentrations

Number	Substrates		Products	
	aspartate (A_o)	α-ketoglutarate (B_o)	glutamate (Q_o)	oxaloacetate (P_o)
1	20	1	10	0
2	7.5	5	20	0
3	0.7	0.3	20	0
4	1	0.5	16	0
5	20	4	15	0
6	11	5	0	0
7	3	2	18	0
8	5	3	15	0
9	20	0.5	0	0
10	1	20	10	0
11	5	7.5	20	0
12	0.3	0.7	20	0
13	0.5	1	16	0
14	4	20	15	0
15	5	11	0	0
16	2	3	18	0
17	3	5	15	0
18	0.5	20	0	0
19	0.05	0.025	5	0
20	10	0.1	0	0
21	0.2	0.1	15	0
22	0.4	0.1	20	0
23	0.025	0.05	5	0
24	0.1	10	0	0
25	0.1	0.2	15	0
26	0.1	0.4	20	0

Approximate initial concentrations (mM) for progress curves in data set. The exact experimental concentrations were determined as described in Section 2.

measured at 340 nm using an extinction coefficient of 6.22×10^3 cm M^{-1} [34] in cuvettes with a 10 mm path length (3.30 ml reaction volume). For limiting substrate concentration between 0.15 to 6.0 mM, NADH oxidation was followed at 380 nm in 2 mm path-length cells (0.75 ml reaction volume). A NADH standard curve at 380 nm was linear to 7.0 mM NADH and had an extinction coefficient of 2.5×10^2 cm M^{-1} (data not shown). All progress curve reactions were initiated with AAT; 50 μl for 10 mm cells and 25 μl for 0.2 mm cells.

2.4. Integrated rate equation

A model for the AAT reaction using the MDH coupled assay is shown in Fig. 1. The derivative rate equation parameters and constants for substrate and malate inhibition from this model were added to the general derivative rate equation ([21–23]; Eq. (1)). The first 16 terms in the denominator are in the general derivative rate equation, and the remaining seven terms in the denominator account for possible substrate or malate inhibition as defined by the model in Fig. 1.

$$\frac{dP}{dt} = \frac{e_o k_{cat} AB}{\begin{aligned} &\frac{J_o}{J_{AB}} + \frac{J_A}{J_{AB}}A + \frac{J_B}{J_{AB}}B + \frac{J_P}{J_{AB}}P + \frac{J_Q}{J_{AB}}Q + \frac{J_{AB}}{J_{AB}}AB \\ &+ \frac{J_{AP}}{J_{AB}}AP + \frac{J_{AQ}}{J_{AB}}AQ + \frac{J_{BP}}{J_{AB}}BP + \frac{J_{BQ}}{J_{AB}}BQ + \frac{J_{PQ}}{J_{AB}}PQ + \frac{J_{ABP}}{J_{AB}}ABP \\ &+ \frac{J_{ABQ}}{J_{AB}}ABQ + \frac{J_{APQ}}{J_{AB}}APQ + \frac{J_{BPO}}{J_{AB}}BPQ + \frac{J_{ABPQ}}{J_{AB}}ABPQ + \frac{J_A}{J_{AB}K_{FA}}A^2 + \frac{J_B}{J_{AB}K_{EB}}B^2 \\ &+ \frac{J_Q}{J_{AB}K_{FQ}}Q^2 + \frac{J_A}{J_{AB}K_{FQ}} + \frac{J_Q}{J_{AB}K_{FA}}AQ + \frac{J_A}{J_{AB}K_{FM}}AM + \frac{J_B}{J_{AB}K_{EM}}BM + \frac{J_Q}{J_{AB}K_{FM}}QM \end{aligned}} \quad (1)$$

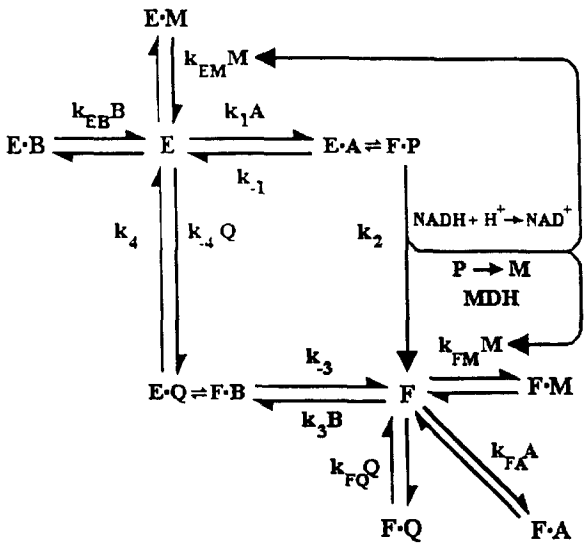

Fig. 1. AAT substitute enzyme mechanism model. The model shows the accepted substituted enzyme mechanism of AAT; in the malate dehydrogenase coupled assay the AAT reaction product oxaloacetate (P) is spontaneously converted to malate. Abbreviations are as defined in notation section. The model was statistically tested for potential inhibition by the coupled assay product, malate, with both forms of the enzyme; PLP (E) and PMP (F). Putative substrate inhibition by aspartate and glutamate with the PMP enzyme form and α-ketoglutarate with the PLP enzyme form were also assessed.

For the model in Fig. 1 the AAT reaction product, oxaloacetate (P), is always zero so terms containing P drop out of the equation. Eq. (1) was integrated as previously described ([21–23]) and terms containing P were eliminated; the resulting integrated rate equation (21 predictors) is presented in tabular format in Table 2 and was used for analysis of all data sets.

2.5. Regression analysis of progress curves

The experimental error in progress curves is in the independent variable, ΔP. In our nonlinear regression analysis the error in ΔP was minimized by iteration which was statistically correct, thus an improvement over the code used in the analysis of LDH where the mean squared error was minimized (error in time; [26]). The mean product error was calculated from $\Sigma(\Delta P_i - \Delta \hat{P}_i)^2/(n - m + 1)$ where n was the total number of time points in the data set and m was the number of constants fit.

For storage of each progress curve, extraction of initial rates, correction of an experimental lag time, and to save computer time, the terms C_f, C_s, C_1, and C_2 were extracted from Eq. (2) below using the nonlinear regression code of Holmes et al. [26] and used *only* to recalculated progress curves.

$$e_0 t = -C_f \ln(1 - \Delta P/A_0) - C_s \ln(1 - \Delta P/B_0) + C_1 \Delta P + 1/2 C_2 \Delta P_2 \quad (2)$$

In contrast to progress curves catalyzed by LDH [26], AAT catalyzed reactions exhibit a lag time after addition of all assay components which varied for each progress curve and adversely affected the regression of Eq. (2) to the progress curve data. A subroutine was incorporated into the code which altered time 0 of the reaction until the minimum mean squared error was found. Residual plots comparing the fit value ($\Delta \hat{P}_i$) to the experimental value (ΔP_i), showed random distribution about 0 and mean squared errors that were typically 10^{-6}, several orders of magnitude below the experimental error, indicating an excellent fit to the data [35].

For each progress curve 8 time points were recalculated from 'C' constants, and the equation (Table 2) was fit to the 26 progress curves for each data set simultaneously by nonlinear regression. In hindsight, the equation represented in tabular format (Table 2) should be fit directly to the progress curve data. 'C' coefficients were used to calculate 8 points/progress curve in 0.1 increments of the limiting substrate concentration (0.1–0.8) which saved computer time. For all points in the 26 progress curve data set, the predictors for the 21 constants in Table 2 were calculated using initial substrate and product concentrations, and ΔP values. This 21 × 208 matrix designated **P**, and the 1 × 208 matrix of the $e_0 t$ observations, **t**, were used to solve the matrix equation $\mathbf{P'PJ} = \mathbf{P't}$ for **J** using Gaussian elimination. The 1 × 21 matrix of kinetic constants, **J**, is shown in Table 2. The multiple regression estimates of the 'J' constants were refined using nonlinear regression to minimize the mean product error. The solution vector for the 'J' constants was refined by successive multiplication by a correction vector $\boldsymbol{X}$ until the mean product error converges. The correction vector $\boldsymbol{X}$ was obtained from the matrix equation $\boldsymbol{e} = \mathbf{D}\boldsymbol{X}$ where $\boldsymbol{e}$ was the fitting error vector $(\Delta P_i - \Delta \hat{P}_i)^2$, and **D** was a matrix of the partial derivative of ΔP with respect to 'J' at each point i. The equation was solved for $\boldsymbol{X}$ using the equation $\mathbf{D'D}\boldsymbol{X} = \mathbf{D'}\boldsymbol{e}$ [36].

Table 2
Tabular representation of the general integrated rate equation with substrate and malate inhibition terms

Parameter	C_f $-\ln(1-\Delta P/A_o)$	C_s $-\ln(1-\Delta P/B_o)$	C_1 ΔP	C_2 $1/2\Delta P$
1. $\frac{1}{k_{cat}}$	0	0	1	0
2. $\frac{J_A}{J_{AB}k_{cat}}$	0	1	0	0
3. $\frac{J_B}{J_{AB}k_{cat}}$	1	0	0	0
4. $\frac{J_P}{J_{AB}k_{cat}}$	$\frac{A_o+P_o}{B_o-A_o}$	$\frac{B_o+P_o}{A_o-B_o}$	0	0
5. $\frac{J_Q}{J_{AB}k_{cat}}$	$\frac{A_o+Q_o}{B_o-A_o}$	$\frac{B_o+Q_o}{A_o-B_o}$	0	0
6. $\frac{J_o}{J_{AB}k_{cat}}$	$\frac{1}{B_o-A_o}$	$\frac{1}{A_o-B_o}$	0	0
7. $\frac{J_{AP}}{J_{AB}k_{cat}}$	0	B_o+P_o	-1	0
8a. $\frac{J_{AQ}}{J_{AB}k_{cat}}$	0	B_o+Q_o	-1	0
8b. $\frac{J_A}{J_{AB}K_{FQ}k_{cat}}$	0	B_o+Q_o	-1	0
8c. $\frac{J_Q}{J_{AB}K_{FA}k_{cat}}$	0	B_o+Q_o	-1	0
9. $\frac{J_{BP}}{J_{AB}k_{cat}}$	A_o+P_o	0	-1	0
10. $\frac{J_{BQ}}{J_{AB}k_{cat}}$	A_o+Q_o	0	-1	0
11. $\frac{J_{PQ}}{J_{AB}k_{cat}}$	$\frac{(A_o+P_o)(A_o+Q_o)}{B_o-A_o}$	$\frac{(B_o+P_o)(B_o+Q_o)}{A_o-B_o}$	1	0
12. $\frac{J_{ABP}}{J_{AB}k_{cat}}$	0	0	P_o	1
13. $\frac{J_{ABQ}}{J_{AB}k_{cat}}$	0	0	Q_o	1
14. $\frac{J_{APQ}}{J_{AB}k_{cat}}$	0	$(B_o+P_o)(B_o+Q_o)$	$B_o+P_o+Q_o$	-1
15. $\frac{J_{BPQ}}{J_{AB}k_{cat}}$	$(A_o+P_o)(A_o+Q_o)$	0	$A_o+P_o+Q_o$	-1
16. $\frac{J_B}{J_{AB}K_{EM}k_{cat}}$	A_o	0	-1	0
17. $\frac{J_A}{J_{AB}K_{FM}k_{cat}}$	0	B_o	-1	0
18. $\frac{J_Q}{J_{AB}K_{FM}k_{cat}}$	$\frac{A_o(A_o+Q_o)}{B_o-A_o}$	$\frac{B_o(B_o+Q_o)}{A_o-B_o}$	1	0
19. $\frac{J_B}{J_{AB}K_{EB}k_{cat}}$	(B_o-A_o)	0	1	0
20. $\frac{J_Q}{J_{AB}K_{FQ}k_{cat}}$	$\frac{(A_o+Q_o)^2}{B_o-A_o}$	$\frac{(B_o+Q_o)^2}{A_o-B_o}$	1	0
21. $\frac{J_A}{J_{AB}K_{FA}k_{cat}}$	0	(A_o-B_o)	1	0

The integrated rate equation factored for 'J' constants. Specific expressions were obtained by multiplying the parameter in column 1 by the corresponding predictors in column 2, 3, 4, or 5 and the specific ΔP term heading these columns; the sum of all terms equals $e_o t$. The results were independent of the assignment of A, B, P, and Q, using only the convention that A and P, and B and Q, correspond in structure. For the AAT reaction A, aspartate; B, α-ketoglutarate; P, oxaloacetate; Q, glutamate; E, PLP enzyme form; F enzyme form; M, the competitive inhibitor malate. Terms 1–5, 6, 8, 9, 11, 13, and 15 correspond to a ternary complex mechanism, and terms 1–5, 7, 10, and 11 correspond to a substituted mechanism.

Table 3
Pearson correlation matrix for integrated rate predictors

	Predictor number										
	1	2	3	5	8	10	16	17	18	19	20
2	0.3										
3	0.3	0.0									
5	0.4	0.6	0.3								
8	0.3	0.8	0.1	0.2							
10	0.3	0.1	0.8	0.2	0.3						
16	0.8	0.1	0.6	−0.2	0.2	0.5					
17	0.8	0.6	0.1	−0.2	0.6	0.2	0.5				
18	0.4	0.5	0.5	0.2	0.8	0.8	0.5	0.5			
19	0.3	−0.3	0.6	−0.2	−0.2	0.2	0.5	0.0	0.0		
20	−0.3	0.3	0.3	0.8	0.4	0.4	−0.1	−0.1	0.4	−0.2	
21	−0.1	0.5	−0.4	−0.1	0.1	−0.3	−0.3	0.2	−0.2	−0.3	−0.1

Each predictor number is defined in Table 2. Correlation values were calculated for the wild-type data set using experimentally determined substrate and product concentrations (approximately those in Table 1).

2.6. Calculation of dissociation constants / initial rate analysis

J constants obtained from nonlinear regressions were used to calculate dissociation constants for binding of substrates, products, or inhibitors using Eqs. (3)–(10) below:

$$K_d(\text{aspartate/PLP form}) = J_b/J_{ab}k_{cat}/(1/k_{cat}) \quad (3)$$

$$K_d(\text{glutamate/PLP form}) = J_{BQ}/J_{AB}k_{cat}/(J_B/J_{AB}k_{cat}) \quad (4)$$

$$K_d(\alpha - \text{ketoglutarate/PMP form}) = J_A/J_{AB}k_{cat}/(1/k_{cat}) \quad (5)$$

$$K_d(\text{aspartate/PMP form}) = J_Q/J_{AB}k_{cat}/(J_Q/J_{AB}K_{FA}k_{cat}) \quad (6)$$

$$K_d(\text{glutamate/PMP form}) = J_Q/J_{AB}k_{cat}/(J_Q/J_{AB}K_{FQ}k_{cat}) \quad (7)$$

$$K_d(\alpha - \text{ketoglutarate/PLP form}) = J_B/J_{AB}k_{cat}/(J_B/J_{AB}K_{EB}k_{cat}) \quad (8)$$

$$K_d(\text{malate/PMP form}) = J_A/J_{AB}k_{cat}/(J_A/J_{AB}K_{FM}k_{cat}) \text{ or } J_Q/J_{AB}k_{cat}/(J_Q/J_{AB}K_{FM}k_{cat}) \quad (9)$$

$$K_d(\text{malate/PLP form}) = J_B/J_{AB}k_{cat}/(J_B/J_{AB}K_{EM}k_{cat}) \quad (10)$$

We have tested our integrated rate analysis by comparison to an initial rate analysis of the same wild-type AAT data set. Initial velocities were calculated for each progress curve using Eq. (11); accuracy was confirmed by superimposing initial rates on progress curves.

$$V_o = C_f/A_o + C_s/B_o + C_1 \quad (11)$$

The Lineweaver–Burk transformation of the substituted enzyme mechanism derivative rate equation with additional substrate and malate inhibition terms were fitted to the initial rate data. 'J' constants were extracted by a multiple regression of a Lineweaver–Burk linear transformation of Eq. (1), using the statistical software, MINITAB (Utah State University VAX).

3. Results

3.1. Choosing substrate and product concentrations

Data sets were designed similar to a standard curve. For each integrated rate equation predictor (e.g., $(1/A_o - B_o)\ln(1 - \Delta P/B_o)$ in Table 2) substrate and product concentrations were chosen such that least one progress curve maximized, minimized, and had an intermediate value of the predictor. Substrate and product concentrations for the 26 progress curves in each enzyme data set are shown in Table 1; experimentally determined substrate and product concentrations were close to these values. The maximum and minimum values of each predictor were limited only by the experimentally attainable substrate and product concentrations and the equilibrium constant of the overall reaction. Predictor values were spread evenly using this method.

Table 4
J constants for wild-type, H193Q and Y70F AATs

Constant	AAT			Units
	wild-type	H193Q	Y70F	
$\frac{1}{k_{cat}}$	1.79 ± 0.03	1.67 ± 0.02	1.82 ± 0.10	s^{-1}
$\frac{J_A}{J_{AB} k_{cat}}$	0.023 ± 0.004	0.027 ± 0.003	0.096 ± 0.021	$mM^{-1}s^{-1}$
$\frac{J_B}{J_{AB} k_{cat}}$	1.01 ± 0.07	1.02 ± 0.05	2.94 ± 0.48	$mM^{-1}s^{-1}$
$\frac{J_Q}{J_{AB} k_{cat}}$	$8.5 \times 10^{-3} \pm 0.6 \times 10^{-3}$	$4.0 \times 10^{-3} \pm 0.3 \times 10^{-3}$	$34 \times 10^{-3} \pm 5 \times 10^{-3}$	$mM^{-1}s^{-1}$
$\frac{J_{BQ}}{J_{AB} k_{cat}}$	0.049 ± 0.004	0.047 ± 0.003	0.082 ± 0.021	s^{-1}
$\frac{J_B}{J_{AB} K_{EM} k_{cat}}$	0.07 ± 0.10	0.025 ± 0.023	–	$mM^{-2}s^{-1}$
$\frac{J_A}{J_{AB} K_{FM} k_{cat}}$	0.21 ± 0.06	0.12 ± 0.16	0.7 ± 1.4	$mM^{-2}s^{-1}$
$\frac{J_Q}{J_{AB} K_{FM} k_{cat}}$	0.020 ± 0.026	0.007 ± 0.045	0.039 ± 0.13	$mM^{-2}s^{-1}$
$\frac{J_B}{J_{AB} K_{EB} k_{cat}}$	0.103 ± 0.006	0.045 ± 0.004	0.20 ± 0.04	$mM^{-2}s^{-1}$
$\frac{J_Q}{J_{AB} K_{FQ} k_{cat}}$	$6.8 \times 10^{-3} \pm 2.0 \times 10^{-3}$	$7.7 \times 10^{-3} \pm 3.0 \times 10^{-3}$	–	$mM^{-2}s^{-1}$

When the reaction conditions were chosen, the limiting substrate must be fully exhausted for analysis with the irreversible integrated rate equations used here. The choice of substrate and product concentrations considered the equilibrium constant of 7.0 for the AAT reaction at pH 7.4, favoring aspartate and α-ketoglutarate [37,38] and the equilibrium constant of 4.29×10^4 for the MDH reaction favoring malate and NAD^+ at physiological pH [39]. The linearity of NADH standard curves was also considered in choosing maximum and minimum limiting substrate concentrations. Since many predictors had $(A_o - B_o)$ or $(B_o - A_o)$ in the denominator, A_o and B_o were maintained at least 1.5-fold different to prevent the approach of these predictors to infinity.

To assess the effect of our revised integrated rate analysis, and choice of experimental substrate and product concentrations we have examined predictor correlation using a Pearson correlation matrix (Table 3). In previous regression analyses from this laboratory several predictors had correlation values above 0.9 [24,26]. Values approaching 1 or -1 indicate a high correlation between the predictors headed by each row and column as defined in Table 2. No correlation value for the wild-type enzyme data set was greater than 0.8 indicating low correlation between predictors.

3.2. Extraction of J constants

Three data sets of twenty-six progress curves for wild-type, H193Q, and Y70F, AATs were analyzed by nonlinear regression of the integrated rate equation factored for Daziel constants (J constants/k_{cat}) as in Table 2. The significant kinetic constants were chosen by a step regression; the nonnegative constants which generated the lowest fitting errors were added to the regression model one at a time until the mean product error was no longer reduced (Table 4). Positive constants which had 't' values lower than 1 (e.g., $J_B/J_{AB}K_{EM}k_{cat}$ and $J_Q J_{AB} K_{FM} k_{cat}$ for the wild-type AAT data set), were added if a reduction in mean product error was observed. The fitting errors for Y70F, H193Q and wild-type data sets were approx. 2% and only constants consistent with a substituted enzyme mechanism were predicted. Standard deviations were calculated using the jack-knife method as previously reported [25] and paralleled those obtained from matrix inversion (data not shown). We have investigated the same weighting schemes used by Holmes et al. [26] (i.e., 1. none, 2. inverse standard deviation, 3. inverse variance, 4. t-weighting, and 5. t^2-weighting). Weighting did not affect the choice of 'J' constants as in the analysis of LDH [26], but did alter the overall fitting error of data sets. Data reported here were obtained using inverse variance weighting which yielded the lowest fitting error.

Table 5
Comparison of kinetic analyses

Constant	Single non-linear regression	Two successive regressions	Initial rate analysis	Units
$\frac{1}{k_{cat}}$	1.79 ± 0.03	0.007 ± 0.007	1.89 ± 0.43	s^{-1}
$\frac{J_A}{J_{AB} k_{cat}}$	0.023 ± 0.004	0.051 ± 0.017	0.07 ± 0.14	$mM^{-1}s^{-1}$
$\frac{J_B}{J_{AB} k_{cat}}$	1.01 ± 0.07	0.055 ± 0.038	1.94 ± 0.22	$mM^{-1}s^{-1}$
$\frac{J_Q}{J_{AB} k_{cat}}$	$8.5 \times 10^{-3} \pm 0.6 \times 10^{-3}$	$7.1 \times 10^{-3} \pm 2.0 \times 10^{-3}$	$2.4 \times 10^{-3} \pm 2.5 \times 10^{-3}$	$mM^{-1}s^{-1}$
$\frac{J_{BQ}}{J_{AB} k_{cat}}$	0.049 ± 0.004	0.0059 ± 0.0020	0.032 ± 0.010	s^{-1}
$\frac{J_B}{J_{AB} K_{EM} k_{cat}}$	0.07 ± 0.10	–	–	$mM^{-2}s^{-1}$
$\frac{J_A}{J_{AB} K_{FM} k_{cat}}$	0.21 ± 0.06	–	–	$mM^{-2}s^{-1}$
$\frac{J_Q}{J_{AB} K_{FM} k_{cat}}$	0.020 ± 0.026	–	–	$mM^{-2}s^{-1}$
$\frac{J_B}{J_{AB} K_{EB} k_{cat}}$	0.103 ± 0.006	0.010 ± 0.002	0.019 ± 0.023	$mM^{-2}s^{-1}$
$\frac{J_Q}{J_{AB} K_{FQ} k_{cat}}$	$3.8 \times 10 \pm 1.2 \times 10$	–	–	$mM^{-2}s^{-1}$

Kinetic constants were extracted from progress curves catalyzed by wild-type AAT by different methods; a 26 curve data set (no repeats) analyzed by a single regression of a integrated rate equation (column 2), a 14 curve data set (in triplicate) fit with the two-regression integrated rate equation method of Holmes et al. ([26]; column 3), or analysis of the data set by the initial rate method. Constants specific to other mechanisms (listed in Table 1) were not included, although tested and found to be insignificant.

3.3. Comparison of kinetic analyses

Kinetic constants extracted from the wild-type AAT data set using the integrated rate analysis of Holmes [26], the revised analysis developed here, and an initial rate analysis were compared (Table 5). Each analysis predicted all substituted mechanism constants, an α-ketoglutarate substrate inhibition constant, and no constants specific to other enzyme mechanisms. Constants for glutamate substrate inhibition, and malate inhibition with the PMP and PLP forms of the enzyme were only predicted in the revised integrated rate analysis, although two malate inhibition terms ($J_Q/J_{AB}K_{FM}k_{cat}$ and $J_B/J_{AB}K_{EM}k_{cat}$) had high t values.

To examine how well constants could be used to recalculate experimental reaction progress curves, theoretical progress curves were calculated using constants determined from each method and the mean product error was assessed. The constants from the single regression analysis yielded a fitting error of approx. 2% compared with 9% for the two regression analysis previously used for LDH [26], and 16.8% for the initial rate analysis. The 7% improvement in fitting error using the revised integrated rate equation analysis drastically improved the prediction of k_{cat} which was poorly predicted using the regression analysis of Holmes [26]; this was a result of the data set design and/or the regression analysis method.

The high 16.8% fitting error observed when progress curves were recalculated using initial rate constants was due largely to inhibition by malate. Under initial rate conditions the concentration of malate (produced from the product oxaloacetate in the MDH coupled reaction) was zero, thus these constants should not be predicted in the initial rate analysis. We have used the malate inhibition terms derived from the single regression integrated rate analysis with constants determined by initial rates to recalculate progress curves. The fitting error was reduced from 16.8 to 5.2% and further addition of the missing glutamate substrate inhibition term caused a minor reduction in fitting error, i.e. 5.0%. The constants extracted by initial rate analysis accurately represent the data. Although the integrated rate analysis fitted the data 3% better than the initial rate analysis, the initial rate analysis uses only 26 initial rates while the integrated rate analysis uses the 8 points from each progress curve (208 points total). The kinetic constants vary up to 5-fold between the three analysis methods suggesting that the reported standard deviations for kinetic constants reflect the precision rather than the accuracy of the method used.

Table 6
Dissociation constants and turnover numbers for AATs

Molecule	Enzyme form	Values and standard deviations		
		E. coli	AAT	
		wild-type	H193Q	Y70F
Productive complexes				
Aspartate	PLP	0.40 ±0.02	1.0 ±0.7	0.95 ±0.10
Glutamate	PLP	21 ±2	22 ±2	36 ±10
α-Ketoglutarate	PMP	0.17 ±0.02	0.084 ±0.009	0.42 ±0.13
Oxaloacetate	PMP	ND	ND	ND
Nonproductive complexes				
Aspartate	PMP	–	–	–
Glutamate	PMP	124 ±37	51 ±20	–
Oxaloacetate	PLP	ND	ND	ND
α-Ketoglutarate	PLP	9.8 ±0.9	23 ±2	15 ±4
Malate	PMP	0.11 ±0.04	0.2 ±0.3	0.09 ±0.03
Malate	PLP	15 ±23	42 ±40	–
k_{cat}		100 ±9	86 ±3	15 ±1

Dissociation constants were calculated from the *J* constants in Table 4 using Eqs. (3)–(10); units are mM. ND indicates kinetic constants that were not accessible using the malate dehydrogenase coupled assay. Turnover numbers (k_{cat}) were calculated from the AAT molecular weight, specific activity, and corrected by the $1/k_{cat}$ value from Table 4. Specific activities for the wild-type, H193Q, and Y70F mutants were 247±22, 197±6, and 39±2 μmol/min per mg, respectively. units for k_{cat} were s^{-1}.

3.4. Analysis of wild-type, H193Q and Y70F AATs

Data sets consisting of 26 progress curves for each the H193Q, Y70F, and wild-type AATs, were analyzed using the revised integrated rate equation analysis and dissociation constants were calculated using Eqs. (3)–(10). The dissociation constants show malate was a very potent inhibitor of the PMP form of wild-type AAT which confirmed the contribution of malate inhibition constants to a large reduction in the fitting error of progress curves recalculated using constants extracted by the initial rate method (Table 6). Malate also bound to the PLP form of the enzyme, although the significance of this constant was questionable due to a high '*t*' value and minimal affect upon the fitting error. A weak but significant glutamate inhibition was also observed.

Comparison of the dissociation constants for the H193Q and wild-type enzymes show minor changes which vary up to 2.5-fold; only a minor change in k_{cat} was observed indicating that the H193Q mutation of AAT has only a minimal affect upon catalysis. Dissociation constants for the Y70F enzyme demonstrated slightly weaker binding of all productive complexes (2–3-fold) and the weak glutamate substrate inhibition was not detected; k_{cat} was 15% of the wild-type enzyme.

4. Discussion

The goals of this study were to improve the analysis of second-order enzymatic reactions using integrated rate equations and demonstrate the utility of this approach in analysis the reactions catalyzed by site-specific mutants of AAT. An important improvement in integrated analysis was factoring the integrated rate equation for '*J*' constants as suggested by Duggleby and Wood [18].

In the analysis of LDH, the integrated rate equation was factored for ΔP terms, and kinetic constants were extracted using two successive regressions [26]. In the first regression '*C*' constants were extracted from Eq. (2) using a nonlinear regression. When two variables are highly correlated such as the logarithmic terms in this equation, matrices become singular and only one constant for the correlated variables can be predicted without advanced statistical techniques such as a

QR decomposition. This problem is not unique to integrated rate analysis but becomes apparent in analysis of the complicated second-order integrated rate equation when factored for ΔP terms.

In the analysis of Holmes [26] the 'C' constants obtained from nonlinear regression of each progress curve were fit to the predictors in columns 2, 3, and 4 of Table 2 to determine the significant kinetic constants. When this analysis method was applied to progress curves catalyzed by AAT, an unrealistic k_{cat} (Table 5) and a relatively large fitting error were observed. The revised single regression analysis has improved the fit of second-order enzymatic reactions demonstrated by a reduced fitting error, a realistic determination of k_{cat}, and detection of previously unreported weak glutamate substrate inhibition, strong malate binding to the PMP enzyme form, and weak malate binding to the PLP enzyme form of well studied wild-type AAT mechanism.

Residue His-193 of AAT is hydrogen bonded consecutively through residues His-189, His-143, and Asp-222 to the pyridine nitrogen of the cofactor [40]. These residues and their positions are conserved among all known AATs. Mutation of Asp-222 for uncharged amino acids dramatically reduces the turnover of aspartate in the PLP half reaction by 10^4 and by 10-fold for the α-ketoglutarate and PMP half reaction [40]. Binding of substrate in both half reactions was diminished up to 5-fold. Mutagenesis of His-143 to alanine had variable affects upon turnover and weakened binding of all substrates up to 8-fold [41]. Here we have studied the H193Q mutant to examine the full extent of this hydrogen bonding network upon binding and catalysis. This mutation caused only small changes in dissociation constants up to 2.5-fold and had a minimal affect on the turnover number, thus the H193Q mutation does not greatly affect catalysis or binding. Considering the previous active site mutational studies, the affects of mutations on AAT catalysis were Asp-222 > His-143 > His-193 as expected.

The Y70F AAT mutant enzyme has a tertiary structure similar to wild-type [42]. This mutant has also demonstrated a lower affinity for the coenzyme presumably due to the loss of a hydrogen bond from the tyrosine phenol to the phosphate of the cofactor [31,43]. Kinetic studies have also shown decreased turnover and binding of all substrates [42,44,45]. Two hypotheses have been presented, one where Tyr-70 has a minor contribution to catalysis for which water can substitute [45], and also the participation in catalysis based on a lowered transition state activation energy (2–3 kcal), and a role for the benzene ring in recognition of the glutamate/α-ketoglutarate substrate pair [42].

All productive complex dissociation constants for the Y70F enzyme increased 1.5–3-fold and k_{cat} was reduced 85% when compared to the wild-type enzyme (Table 6), similar to that reported [42]. The dissociation constants for nonproductive complexes did not change significantly, although glutamate substrate inhibition and malate inhibition of the PLP enzymatic form were not detected for this mutant. For the wild-type enzyme these constants were very weak (glutamate) or not statistically significant (malate).

Advances in computational power and commercial software have made integrated rate analysis usable to all biochemists. Since this study was completed the software, Sigmaplot (Jandel Scientific; Corte Madera, CA) can accommodate nonlinear regression analysis with many variables and large matrices such that progress curve data from a second-order enzymatic reaction can be analyzed using the general integrated rate equation.

In summary, our integrated rate analysis was revised by factoring the integrated rate equation for J constants and fitting all progress curves simultaneously which resulted in better fitting errors. Integrated rate analysis of wild-type, H193Q, and Y70F AATs has demonstrated a strong inhibition due to malate binding to the PMP form of the enzyme. The kinetic constants determined for wild-type and Tyr-70 enzyme were similar to those previously reported indicating the validity of integrated rate analysis. The minimal changes in kinetic constants observed for the H193Q mutant AAT suggests that catalytic effects of the electronic communication of the cofactor extending through Asp-222, His-143, and His-189, does not extend to His-193. This study demonstrates the utility of integrated rate analysis in extracting kinetic constants from complicated enzymatic systems and analyzing site-directed mutants.

Acknowledgements

This work was supported in part by National Institutes of Health grant GM34065. We thank Dr. Jack Kirsch, Dr. Jonathan Goldberg and Dr. Michael Toney for the wild-type AAT and AAT mutant bearing strains; Dr. Jack Kirsch and Dr. Aparna Kolhekar for critical review of the manuscript. We also wish to acknowledge Dr. Elizabeth Boeker, who unfortunately passed away and did not see the completed publication of her work on integrated rate equations; Dr. Boeker was not involved in preparation of this manuscript.

References

[1] Henri, V. (1902) C.R. Acad. Sci. Paris 135, 916–919.
[2] Michaelis, L. and Menten, M.L. (1913) Biochem. Z. 49, 333–369.

[3] Walker, A.C. and Schmidt, C.L.A. (1944) Arch. Biochem. Biophys. 5, 445–467.
[4] Huang, H.T. and Neimann, C. (1951) J. Am. Chem. Soc. 73, 1541–1548.
[5] Schønheyder, F. (1952) Biochem. J. 50, 378–384.
[6] Alberty, R.A. (1953) J. Am. Chem. Soc. 75, 1928–1932.
[7] Alberty, R.A. (1958) Adv. Enzymol. 17, 1–64.
[8] Cleland, W.W. (1963) Biochem. Biophys. Acta 67, 104–137.
[9] Cleland, W.W. (1963) Biochem. Biophys. Acta 67, 173–187.
[10] Cleland, W.W. (1963) Biochem. Biophys. Acta 67, 188–196.
[11] Bates, D.J. and Frieden, C. (1973) J. Biol. Chem. 248, 7885–7890.
[12] Duggleby, R.G. and Morrison, J.F. (1977) Biochem. Biophys. Acta 481, 297–312.
[13] Duggleby, R.G. and Morrison, J.F. (1978) Biochem. Biophys. Acta 526, 398–409.
[14] Duggleby, R.G. and Morrison, J.F. (1979) Biochem. Biophys. Acta 568, 357–362.
[15] Vandenberg, J.I., Kuchel, P.W. and King, G.F. (1986) Anal. Biochem. 155, 38–44.
[16] Gray, R.J. and Duggleby, R.G. Biochem. J. 257, (1989) 419–424.
[17] Duggleby, R.G. and Nash, J.C. (1989) Biochem. J. 257, 57–64.
[18] Duggleby, R.G. and Wood, C. (1989) Biochem. J. 258, 397–402.
[19] Szedlacsek, S.E., Ostafe, V., Duggleby, R.G. and Vlad, M.O. (1990) Biochem. J. 265, 647–653.
[20] Franco, R., Aran, J.M. and Canela, E.I. (1991) Biochem. J. 274, 509–511.
[21] Boeker, E.A. (1984) Experientia 40, 453–456.
[22] Boeker, E.A. (1984) Biochem. J. 223, 15–22.
[23] Boeker, E.A. (1985) Biochem. J. 226, 29–35.
[24] Cox, T.T. and Boeker, E.A. (1987) Biochem. J. 245, 59–65.
[25] Boeker, E.A. (1987) Biochem. J. 245, 67–74.
[26] Holmes, L.D., Schiller, M.R. and Boeker, E.A. (1993) Experientia 49, 893–901.
[27] Nomenclature Committee of the International Union of Biochemistry (NC-IUB) (1982) Eur. J. Biochem. 128, 281–291.
[28] Karmen, A. (1955) J. Clin. Invest. 341, 131–138.
[29] Cronin, C.N. and Kirsch, J.F., Biochemistry 27 (1988) 4572–4579.
[30] Toney, M.D. and Kirsch, J.F. (1989) Science 243, 1485–1488.
[31] Toney, M.D. and Kirsch, J.F. (1987) J. Biol. Chem. 262, 12403–12405.
[32] Decker, L.A. (1977) Worthington Enzymes Manual, Worthington Biochemical Corp., Freehold, NJ.
[33] Selwyn, M.J. (1965) Biochem. Biophys. Acta 105, 193–195.
[34] Segal, I.H. (1976) Biochemical Calculations, 2nd Ed., Wiley, New York.
[35] Draper N.R. and Smith, H. (1981) Applied Regression Analysis, 2nd Ed., Wiley, New York.
[36] Neter, J. and Wasserman, W. (1974) Applied Linear and Statistical Models Irwin, Homewood, IL.
[37] Velick, V.F. and Vavra, J. (1962) J. Biol. Chem. 237, 2109–2122.
[38] Henson, C.P. and Cleland, W.W. (1964) Biochemistry 3, 338–345.
[39] Ochoa, S., (1955) in Methods in Enzymology, (Colowick, S.P. and Kaplan, N.O., eds.), Vol. 1, pp. 735–739, Academic Press, New York.
[40] Yano, T., Kuramitsu, S., Tanase, S., Yoshimasa, M. and Kagamiyama, H. (1992) Biochemistry 31, 5878–5887.
[41] Yano, T., Kuramitsu, S., Tanase, S., Yoshimasa, M., Hiiromi, K. and Kagamiyama, H. (1991) J. Biol. Chem. 266, 6079–6085.
[42] Inoue, Y., Kuramitsu, S., Okamoto, A., Hirotsu, K, Higuchi, T. and Kagamiyama, H. (1991) Biochemistry 30, 7796–7801.
[43] Toney, M.D. and Kirsch, J.F. (1991) Biochemistry 30, 7456–7461.
[44] Kirsch, J.F., Finlayson, W.L., Toney, M.D. and Cronin, C.N. (1987) in Biochemistry of Vitamin B_6 (Korpela, T., and Christen, P., eds.), pp. 59–67, Birkhauser Verlag, Basel.
[45] Toney, M.D. and Kirsch, J.F. (1991) Biochemistry 30, 7461–7466.